Rates and Mechanism of Oxidative Two-Electron-Transfer-Induced *cis* to *trans* Isomerization of the Nitrile Complex [ReCl(NCC$_6$H$_4$Me-4)(Ph$_2$PCH$_2$CH$_2$PPh$_2$)$_2$]

M. Fátima C. Guedes da Silva, João J. R. Fraústo da Silva, and Armando J. L. Pombeiro*

Centro de Química Estrutural, Complexo I, Instituto Superior Técnico, Av. Rovisco Pais, 1096 Lisboa Codex, Portugal

Christian Amatore* and Jean-Noël Verpeaux*

Ecole Normale Supérieure, Département de Chimie, URA CNRS 1679, 24 rue Lhomond, F-75231 Paris Cedex 05, France

Received March 1, 1994®

In an aprotic medium and at a platinum electrode, *cis*-[ReCl(NCC$_6$H$_4$Me-4)(Ph$_2$PCH$_2$CH$_2$PPh$_2$)$_2$], a thermally stable 18-electron complex, is oxidized *via* two successive one-electron transfers, respectively, to 17- and 16-electron configurations. The 17-electron cation radical is found to be stable even within the time scale of preparative electrolysis and can be reduced back to the 18-electron parent complex. Conversely, the 16-electron dicationic complex is shown to undergo a facile isomerization to its *trans* isomer, a process that occurs readily during the time scale of cyclic voltammetry. Full quantitative kinetic analysis of the voltammetric behavior is presented and allows the determination of the two pertinent first-order rate constants and therefore of the equilibrium constant of the reversible *cis* to *trans* isomerization reaction that occurs at the level of the 16-electron complexes.

Introduction

Given the recognized dependence of the relative stability and redox behavior of geometrical isomers of octahedral-type complexes on their electronic configuration, electrochemistry provides convenient tools for such investigation as well as for the study of their possible interconversion, matters which have been the subject of considerable debate.[1–9] In particular, semiempirical predictions[1] of the redox potentials, theoretical calculations,[2–4] and experimental observations on some bis(dinitrogen),[5,6] dicarbonyl,[7] or dinitrile[8] complexes are conflicting in a number of cases.

Following our interest[10] in the activation of small unsaturated molecules, we now extend the electrochemical study to the mononitrile complex *cis*-[ReCl(NCC$_6$H$_4$-Me-4)(dppe)$_2$] (form *a*) which, in contrast with the above

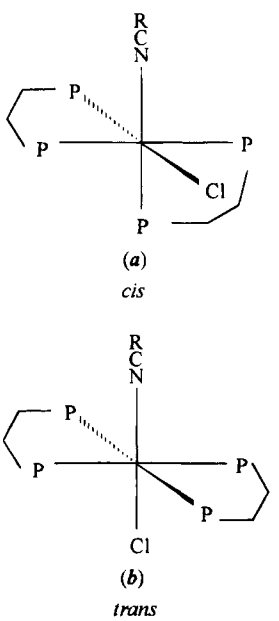

cases (*viz.* with two weak (N_2), two strong (CO), or two moderate (NCR) π-acceptors), presents a strong electron donor (Cl) and a π-acceptor (NCR) ligand at a coordinating phosphinic metal center. Geometrical isomerization induced by two-electron charge transfer is observed at the level of the 16-electron complex, and a detailed mechanistic study of such a process is presented. Moreover, that complex—which has been prepared by reaction of *trans*-[ReCl(N_2)(dppe)$_2$] with the appropriate nitrile in toluene—provides the second known example

* To whom correspondence should be addressed.
® Abstract published in *Advance ACS Abstracts,* August 15, 1994.

(1) Bursten, B. E. *J. Am. Chem. Soc.* **1982,** *104,* 1299.
(2) Dubois, D. L.; Hoffmann, R. *Nouv. J. Chim.* **1977,** *1,* 479.
(3) Murrell, J. N.; Al-Derzi, A.; Leigh, G. J.; Guest, M. F. *J. Chem. Soc., Dalton Trans.* **1980,** 1425.
(4) Mingos, D. M. P. *J. Organomet. Chem.* **1979,** *179,* C29.
(5) George, T. A.; Hayes, R. K.; Mohammed, M. Y.; Pickett, C. J. *Inorg. Chem.* **1989,** *28,* 3269.
(6) George, T. A.; Debord, J. R. D.; Kaul, B. B.; Pickett, C. J.; Rose, D. J. *Inorg. Chem.* **1992,** *31,* 1295.
(7) Bond, A. M.; Cotton, R.; Jackowski, J. J. *Inorg. Chem.* **1975,** *14,* 274. Wimmer, F. L.; Snow, M. R.; Bond, A. M. *Inorg. Chem.* **1974,** *13,* 1617.
(8) Guedes da Silva, M. F. C.; Duarte, M. T.; Galvão, A. M.; Fraústo da Silva, J. J. R.; Pombeiro, A. J. L. *J. Organomet. Chem.* **1992,** *433,* C14.
(9) Ohsaka, T.; Oyama, N.; Yamaguchi, S.; Matsuda, H. *Bull. Chem. Soc. Jpn.* **1981,** *54,* 2475. Rader, R. A.; McMillin, D. R. *Inorg. Chem.* **1979,** *18,* 545.
(10) Pombeiro, A. J. L. *Inorg. Chim. Acta* **1992,** *198–200,* 179. Pombeiro, A. J. L.; Richards, R. L. *Coord. Chem. Rev.* **1990,** *104,* 13 and references cited therein.

0276-7333/94/2313-3943$04.50/0

of a *cis* isomer of rhenium complexes of the general type $[ReL_2L'_4]$[8] (where the two L ligands can be either identical or different from each other and L′ is commonly a phosphine or represents half of a diphosphine), for which the *trans* geometry has been well documented.[10]

Results and Discussion

Delineation of the General Mechanistic Features. In THF, cyclic voltammetry of the *trans* isomer of $[ReCl(NCC_6H_4Me\text{-}4)(dppe)_2]$ (form *b*) consists of two successive one-electron chemically reversible waves featuring the respective formation of the stable cationic and dicationic species (*vide infra*), at the potentials of $E°(trans^{+/0}) = -0.31$ V *vs* SCE and $E°(trans^{2+/+}) = 0.67$ V *vs* SCE.[11] In agreement with this description, controlled-potential electrolysis (CPE) on the plateau of the first wave consumes 1 faraday/mol to afford a species which was isolated and shown to be the stable $trans^+$ complex by comparison of its properties with those of a genuine sample prepared chemically (see the Experimental Section). Similarly, CPE of the $trans^0$ complex solution, performed on the plateau of the second wave, consumes 2 faradays/mol. However, despite the completely chemically reversible character of the voltammogram of the $trans^{2+/+}$ couple, only minor yields of the $trans^{2+}$ species were achieved; this latter species was obtained together with a mixture of its degradation products that could not be isolated or characterized.

$$trans^0 \underset{+e^-}{\overset{-e^-}{\rightleftharpoons}} trans^+ \underset{+e^-}{\overset{-e^-}{\rightleftharpoons}} trans^{2+} \xrightarrow{\text{slow (CPE)}} \text{degradation} \quad (1)$$

At high scan rates ($v \gg 2$ V s^{-1}) the cyclic voltammetry of the *cis* isomer is very reminiscent of that of the *trans* isomer, showing two successive one-electron chemically reversible waves[11] at $E°(cis^{+/0}) = -0.13$ V *vs* SCE and $E°(cis^{2+/+}) = 0.70$ V *vs* SCE. At lower scan rates ($v < 2$ V s^{-1}) the first wave remains fully reversible, provided that the potential scan is inverted between the two waves. However, for the same low scan rates but when the potential scan is inverted after the second wave, the reduction part of the second wave becomes ill-defined and corresponds to the overlapping of the reduction peaks of the cis^{2+} and $trans^{2+}$ species (compare Figure 1a). At even lower scan rates (compare Figure 1b,c) only the reduction peak of the $trans^{2+}$ species is observed. This indicates that a *cis* to *trans* isomerization takes place at the level of the cis^{2+} dication. However, due to the strong overlapping between the reduction waves of the cis^{2+} and $trans^{2+}$ dications (Figure 1a), a precise characterization of the isomerization process as well as a quantitative evaluation of its kinetics is almost impossible on the basis of these waves only.[12]

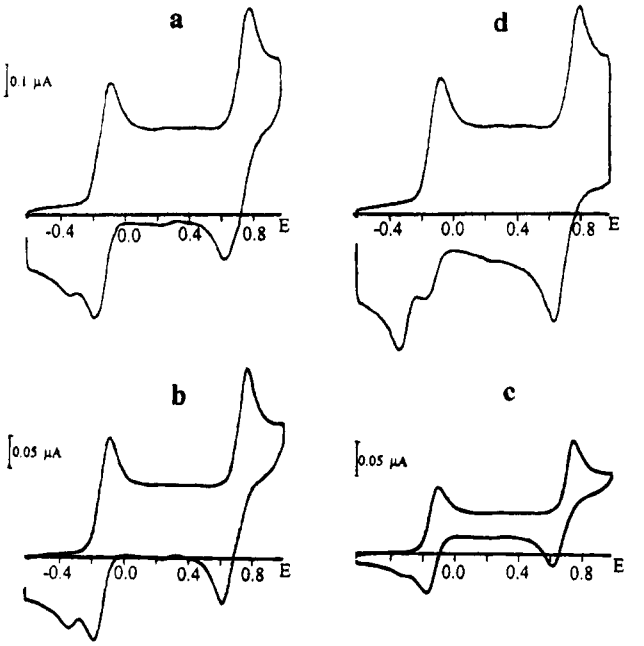

Figure 1. Cyclic voltammetry of the cis^0 isomer (0.96 mM, in THF with 0.2 M $[NBu_4][BF_4]$) at 0 °C. A platinum disk electrode (0.5 mm diameter) was used; potentials are given in V *vs* SCE. San rate: 0.8 (a), 0.2 (b), and 0.05 V s^{-1} (c). In (d), a scan rate of 0.8 V s^{-1} was used as in (a), yet the potential was held for 10 s at the plateau of the cis^+ oxidation wave before the return scan was performed (see text).

This becomes easier when the backward scan is examined in the region where the reduction of the monocations take place. Indeed, one observes then the two well-separated reduction peaks of cis^+ and $trans^+$ (compare Figure 1a). Moreover, at any scan rate ($0.05 \le v \le 5$ V s^{-1}) and any concentration (*ca.* 1−3 mM) examined in this study, the sum of the peak currents of both reduction peaks (*viz.* $i_p(trans^{+/0}) + i_p(cis^{+/0})$) is found to be equal, within the limits (±5%) of its measurement, to the peak current of the cis^0 oxidation wave (*viz.* $i_p(cis^{0/+})$).[13a] Since this is akin to a check of mass conservation,[13b] it establishes that the isomerization process, taking place at the level of the dicationic species, occurs without a significant involvement of any other chemical process within the time scale of cyclic voltammetry.

In conformity with these results based on cyclic voltammetry, CPE at the first oxidation wave of the *cis* isomer consumes 1 faraday/mol and affords stoichiometrically the corresponding stable cation cis^+; conversely, CPE performed at the second wave of a cis^0 solution involves 2 faradays/mol and affords the same

(11) Heterogeneous electron transfers are fast, as evidenced by peak-to-peak separation ($\Delta E_p = E_{pa} - E_{pc}$) and half-width ($\Delta E_{p/2} = E_{pa} - E_{p/2a}$) values identical with those obtained for ferrocene under the same experimental conditions. For example, at $v = 0.1$ V s^{-1}, $\Delta E_p(trans^{+/0}) = 70 \pm 5$ mV, $\Delta E_p(trans^{2+/+}) = 60 \pm 5$ mV, and $\Delta E_p(cis^{+/0}) = 72 \pm 5$ mV. For the $cis^{2+/+}$ wave ΔE_p could not be measured at these scan rates because of the isomerization reaction; however, its $\Delta E_{p/2}$ value (35 ± 5 mV at $v = 0.1$ V s^{-1}) was close to those of the three other waves considered here as apparent in Figure 1a−c.

(12) Such a kinetic investigation is formally possible. However, to lead to an accurate kinetic description of the mechanism at hand, it would presuppose a complete knowledge of other extraneous effects that also affect the wave shapes (*e.g.*, ohmic drop, background currents, etc.).

(13) (a) See Experimental Section and Figure 3b for the determination of the peak currents. (b) Since all waves are nearly Nernstian, the proportionality relationship[14] between their peak current and the concentration of the species near the electrode vicinity involves the same proportionality factor.

(14) Bard, A. J.; Faulkner, L. R. *Electrochemical Methods*; Wiley: New York, 1980.

product distribution as obtained after CPE on the second wave of the *trans*^{0} isomer (eq 2). This series of

$$cis^0 \underset{+e^-}{\overset{-e^-}{\rightleftharpoons}} cis^+ \underset{+e^-}{\overset{-e^-}{\rightleftharpoons}} cis^{2+} \xrightarrow{k} trans^{2+} \xrightarrow{\text{slow (CPE)}} \text{degradation}) \quad (2)$$

experiments (*viz.* voltammetry and CPE at each set of waves) indicates that isomerization of the *cis* species into the *trans* ones occurs at the level of the dications, as featured in Scheme 1.

Scheme 1

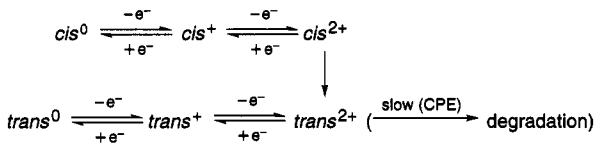

However, the system at hand appears more intricate than that suggested by Scheme 1. This is evidenced by the evolution of the voltammograms in Figure 1 as a function of the scan rate. On the one hand, and in agreement with the formulation in Scheme 1, at fast scan rates (*e.g.* at 0.8 V s^{-1} in Figure 1a) the reduction wave located at *ca.* 0.6 V is broad because it corresponds to the overlapping reduction waves of *cis*$^{2+}$ and *trans*$^{2+}$ species, featuring an incomplete isomerization because of the short time scale used; at slower scan rates (*e.g.* for 0.2 and 0.05 V s^{-1} in parts b and c of Figure 1, respectively) this wave becomes sharp and features the reduction of *trans*$^{2+}$ only, demonstrating that the *cis*$^{2+}$ to *trans*$^{2+}$ isomerization is complete within these longer time scales. On the other hand, and despite the above observations at the second waves, it is seen from the CVs at 0.2 and 0.05 V s^{-1} that a significant reduction wave is still observed for the *cis*$^+$ isomer at *ca.* −0.2 V. Moreover, when the scan rate is decreased (compare parts b and c of Figure 1), the size of the *cis*$^+$ reduction wave increases at the expense of that of the *trans*$^+$ wave. This puzzling behavior is illustrated quantitatively in Figure 2a, in the form of a plot of $\varrho = i_p(trans^{+/0})/i_p(cis^{0/+}) = i_p(trans^{+/0})/[i_p(trans^{+/0}) + i_p(cis^{+/0})]$, *viz.* of the variations of the yield in *trans*$^+$ species, as a function of the scan rate v, for several concentrations used in this study.[15] It is seen from the right-hand side of this plot that this yield increases upon decreasing the scan rate, in agreement with the above qualitative observations based on the reduction waves of the dications. Yet for scan rates below *ca.* 0.3 V s^{-1} (left-hand side of Figure 2a), this yield decreases upon decreasing the scan rate, in contradiction with expectations based on the formulation in Scheme 1.

Part of this apparently puzzling behavior could be thought to be accounted for by considering the effect of diffusion only. Indeed, due to the large potential separation (*ca.* 1 V) between the dicationic and monocationic sets of reduction waves, the content of the diffusion layer is significantly affected by diffusion of reactants and products during the backward potential scan. Thus, while the potential is scanned over the *ca.* 1 V gap separating the two sets of waves, significant fractions of the *trans*$^{2+}$ species that were formed in the potential range where the second waves are observed and of the *trans*$^+$ species that result from *trans*$^{2+}$ reduction at the electrode surface are evacuated from the electrode vicinity by their diffusion toward the bulk of the solution. Simultaneously, these diffusional losses are exactly compensated by diffusion of the reactant *cis*^{0} species from the bulk of the solution toward the electrode surface, where it is immediately oxidized into the stable *cis*$^+$ cation. Therefore, such diffusional losses explain qualitatively that the extent of isomerization as measured by ϱ values in Figure 2a, *viz.* at the level of the monocation reduction waves, appears necessarily less than its "true" extent, as could be determined on the basis of the dication reduction waves. However, as will be made clear in the following, these losses cannot explain the nonmonotonous variations of ϱ as a function of the scan rate that are shown in Figure 2a.

Indeed, such a classical effect of diffusion depends only on the extension of the potential scan and not on the scan rate. It is only a function of the relative time duration of the period in which formation of *trans*$^{2+}$ occurs to that in which diffusional losses and replenishment of the diffusion layer occurs. The ratio of these two time durations is obviously independent of the scan rate and, for a given system, depends only on the inversion potential. Therefore, these diffusional contributions should conserve the monotonous nature of the variations of ϱ as a function of the scan rate. This is further confirmed by the comparison of the data in Figure 2a with the working curve (solid line in Figure 2a) relative to the mechanism in Scheme 1 (*vide infra*) which takes into account all these diffusional contributions. The first conclusion drawn from this comparison is that the data on the righ-hand side of Figure 2a (above *ca.* 0.3 V s^{-1}, *viz.* those that decay upon increas-

(15) During the earliest stages of this study, we observed an apparent dependence of ϱ values on concentration, which was rationalized by considering bimolecular rate laws for the *cis* to *trans* isomerization. However, these dependences were eventually shown to arise from the presence of an impurity (whose concentration in the solutions investigated was then proportional to that of the *cis*^{0} complex) that catalyzes the isomerization process, resulting in conversion rates about 5 times larger than those reported here. These effects could not be reproduced upon investigation of new and fully purified synthetic batches of *cis*^{0} complex. The nature of the impurity responsible for these catalytic effects is still unknown and is under investigation.

(16) The thickness of the diffusion layer created during an electrochemical perturbation of duration θ is proportional to $(D\theta)^{1/2}$, where D is the diffusion coefficient of the species considered.[14] Thus during the "hold" duration period, θ_{hold}, a diffusion layer of thickness proportional to $(D\theta_{hold})^{1/2}$ expands from the electrode surface toward the solution bulk. Upon cessation of the hold period, and during the time θ_{scan} required to scan the potential between the two sets of reduction waves relative to dications and monocations, another diffusion layer of thickness $(D\theta_{scan})^{1/2}$ builds up, starting from the solution end of the former and expanding toward the electrode surface. Finally, when the monocation reduction waves are scanned, which requires a duration time θ_{wave}, a third diffusion layer of thickness $(D\theta_{wave})^{1/2}$ builds up from the electrode surface toward the solution. The relative amount of *cis*$^+$ and *trans*$^+$ shown by the relative importance of their reduction peak currents reflects the composition of this third diffusion layer. It is thus understood that, provided that $(D\theta_{wave})^{1/2} < (D\theta_{hold})^{1/2} - (D\theta_{scan})^{1/2}$, the composition of the solution in the third diffusion layer cannot be affected by that which has been created during the period in which the potential was scanned between the two sets of reduction waves. Under these conditions, the reduction waves of the monocations represent the chemical fate of the solution without interference of diffusional leaks. For example, at 0.8 V s^{-1} (Figure 1d) one has $\theta_{hold} \approx 10$ s, $\theta_{scan} \approx 1$ s, and $\theta_{wave} \approx 0.2$ s; therefore, $(\theta_{wave})^{1/2} \approx 0.5$ s$^{1/2} < 2.2$ s$^{1/2} \approx (D\theta_{hold})^{1/2} - (D\theta_{scan})^{1/2}$. Conversely, for the same scan rate, but without imposition on purpose of a hold period (*viz.* as in Figure 1a), one has $\theta_{hold} \approx 0.5$ s, since this corresponds approximately to the time duration where the potential lies on the plateaus of the monocation oxidation waves. Thus, the above inequality is no longer verified: $(\theta_{wave})^{1/2} \approx 0.5$ s$^{1/2}$, whereas $(D\theta_{hold})^{1/2} - (D\theta_{scan})^{1/2} \approx -0.8$ s$^{1/2} < 0$. Thus, the diffusion layer created during the scanning period perturbs entirely the measurements based on the monocation reduction waves.

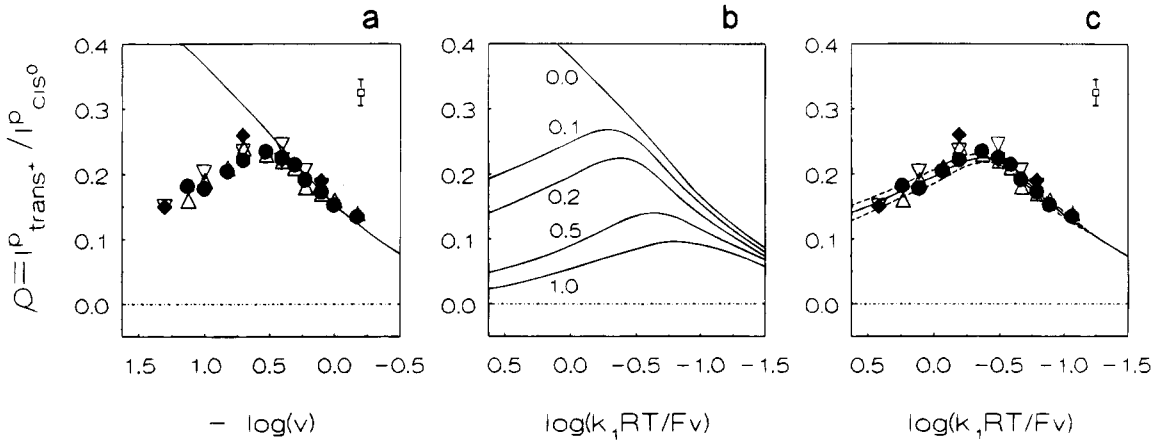

Figure 2. Experimental (a) and theoretical (b) variations of $\varrho = i_p(trans^{+/0})/i_p(cis^{0/+}) = i_p(trans^{+/0})/[i_p(trans^{+/0}) + i_p(cis^{+/0})]$ as a function of scan rate (v) and concentration (●, 0.95 mM; △, 2.0 mM; ▽, 2.6 mM; ♦, 0.96 mM; from CVs shown in Figure 1) at 0 °C. In (a) the solid line corresponds to the working curve for an irreversible isomerization ($k_2 = 0$ and $k_1 = 4.0$ s^{-1}). In (b) several working curves corresponding to different values of k_2/k_1 (as indicated by numbers on each curve) are shown for the mechanism in Scheme 3, considering also the homogeneous electron transfer in eqs 3−8. In (c) the experimental data shown in (a) are superimposed on the working curve determined for $k_1 = 5.6$ s^{-1} and $k_2/k_1 = 0.18$ (note that working curves for $k_2/k_1 = 0.19$ and $k_2/k_1 = 0.17$ are also shown as dashed lines for comparison). In (a,c) error bars on experimental data are shown in the top right corner. Note that in (a) a "−log v" scale is used, whereas in (b,c) a dimensionless scale is used instead. For any given value of k_1, the two scales are identical except for a constant translation of log (k_1RT/F).

ing the scan rate) roughly match the predictions of the working curve determined for Scheme 1 considering an isomerization rate constant $k = 4.0 \pm 0.2$ s^{-1} (eq 2). A second conclusion is that the working curve varies monotonously as a function of the scan rate, in agreement with our statement above, and in disagreement with the experimental observations in Figure 2a (below *ca.* 0.3 V s^{-1}).

The fact that this nonmonotonous behavior does not originate from any diffusional effects can also be checked experimentally, *viz.* independently of any presupposed reaction mechanism, by modifying the relative time durations of the periods in which the *trans* species is produced to that where *trans* species are evacuated from the electrode vicinity by diffusion. This may be performed by interrupting the potential scan on the plateau of the cis^+ oxidation wave, *viz.* by holding the potential at 1.0 V, for a duration that greatly exceeds that of the time span required to scan the potential between the dication and monocation reduction waves.[16] After the potential hold period, the potential scan is resumed toward negative potentials using the same scan rate that was used for the forward scan. Such a procedure ensures that diffusion during the backward scan cannot affect significantly the *cis/trans* composition of the diffusion layer.[16] It is seen in Figure 1d that all cis^{2+} has been converted into $trans^{2+}$ during the "hold" period. This quantitative conversion is evidenced by the observation of only a thin reduction peak for the latter species without a significant contribution of the reduction wave of the former. In contrast, a reduction peak is again observable for the cis^+ species at *ca.* −0.2 V. The observation of a cis^+ reduction wave under these experimental conditions establishes that a chemical

Scheme 2

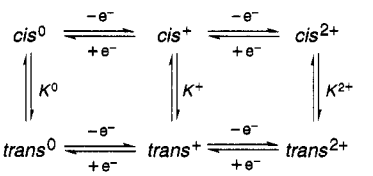

reaction converting the *trans* isomer back to the *cis* isomer must be considered. In the following section we wish to identify the nature of this chemical step.

First, from the concentration independence of the data in Figure 2a,[15] we know that only first-order (or *pseudo*-first-order) reactions have to be considered for the chemical steps.[17,18] Indeed, it is seen from the plot in Figure 2a that data obtained over a nearly 3-fold increase in concentration overlap within the accuracy of their determinations. Also, because of charge conservation, any overall isomerization step must conserve the charge character (neutral, monocation, or dication) of the precursor species. Therefore, without considering at this stage the necessary involvement of homogeneous electron-transfer steps (*vide infra*), the most general kinetic situation that may arise can be described by the classical form of a double *square scheme* given in Scheme 2, where all steps indicated are first (or *pseudo*-first) order in the relevant species.

We know from the CPE experiments reported above that no isomerization may occur at the level of neutral or monocationic species even over the long time durations required for CPE (*vide infra*). We are therefore led to the conclusion that the only sequence that is compatible with all data at hand is that featured in Scheme 3, *i.e.* involving a reversible isomerization at the level of dications.

In the following we wish to investigate quantitatively the above mechanism in order to substantiate it on detailed kinetic grounds.

(17) A second-order kinetic process would impose overlapping of the data when plotted as a function of (C^0/v), C^0 being the concentration of the cis^0 reactant, rather than when plotted as a function of v as in Figure 2a. Due to the logarithmic scale used in Figure 2a, plotting data obeying second-order kinetics should correspond to a shift of *ca.* 0.44 logarithmic unit between the data obtained for $C^0 = 0.95$ and 2.6 mM. Such a shift is clearly beyond the experimental uncertainty (*vide infra* for the effect of bimolecular electron transfer[21]).

(18) Amatore, C. In *Organic Electrochemistry*; Baizer, M., Lund, H., Eds.; Marcel Dekker: New York, 1991; Chapter 2.

Scheme 3

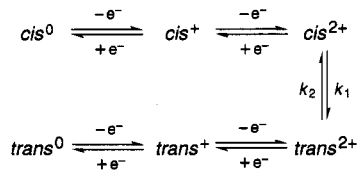

Quantitative Kinetic Investigation of the Mechanism in Scheme 3. The simplified formulation in Scheme 3 does not take into account all the homogeneous electron-transfer reactions involving the species represented. Indeed, since four redox couples are involved, each one with nearly Nernstian electron-transfer kinetics, the corresponding species are also necessarily involved in a sequence of six fast homogeneous electron transfers. Some of these electron-transfer steps are reversible, while the others may be considered as irreversible. Indeed, the equilibrium constant of each homogeneous electron transfer is imposed by the relative values of the standard potentials of the two redox couples involved. Hence, one has (at 273 K)

$$cis^+ + trans^0 \rightleftharpoons cis^0 + trans^+ \quad K_3 = 2.1 \times 10^3 \quad (3)$$

$$cis^{2+} + trans^+ \rightleftharpoons cis^+ + trans^{2+} \quad K_4 = 3.6 \quad (4)$$

$$cis^{2+} + cis^0 \rightarrow cis^+ + cis^+ \quad K_5 \approx 2.1 \times 10^{15} \quad (5)$$

$$trans^{2+} + trans^0 \rightarrow trans^+ + trans^+ \quad K_6 \approx 1.3 \times 10^{18} \quad (6)$$

$$cis^{2+} + trans^0 \rightarrow cis^+ + trans^+ \quad K_7 \approx 4.5 \times 10^{18} \quad (7)$$

$$trans^{2+} + cis^0 \rightarrow trans^+ + cis^+ \quad K_8 \approx 6.0 \times 10^{14} \quad (8)$$

From a kinetic point of view, the two electron transfers in eqs 3 and 4 must be considered as being extremely fast in both directions. Indeed, they involve redox couples with almost Nernstian heterogeneous electron-transfer kinetics; therefore, their rate constants are expected to be nearly controlled by the diffusion of products (eq 3) or products and reactants (eq 4) accordingly.[19] For example, reaction 3 is expected to have a forward rate constant close to the diffusion limit (*viz. ca.* 10^9–10^{10} M^{-1} s^{-1}), implying a backward rate constant in the range of 5×10^5 to 5×10^6 M^{-1} s^{-1} in order to fulfill the thermodynamic condition $K_3 = k_{+3}/k_{-3} = 2.1 \times 10^3$.[19] Similarly, the electron transfer in eq 4 is expected to have both of its rate constants close to the diffusion limit. Such diffusion-limit estimations of rate constants are even more accurate for the electron transfers in forward eqs 5–8 owing to their extremely large exergonic character.[19] Conversely, the rate constants of the backward reactions of electron transfers in eqs 5–8 are extremely small. Indeed, because of thermodynamics (since $K_n = k_{+n}/k_{-n}$) the fastest reaction, *i.e.* that with the smallest K value (eq 8), has a rate constant k_{-8} smaller than 2×10^{-5} M^{-1} s^{-1}. Since the concentrations used in this study are in the millimolar range, all homogeneous electron transfers in eqs 3–8 correspond to extremely short half-conversion times (below 2 ms for the backward reaction of eq 3 and below 1 μs to 0.1 μs for all the other reactions); *i.e.*, they are considerably faster than any isomerization reaction involved in Scheme 3.[21] Conversely, the backward reactions of eqs 5–8 can be omitted since they correspond to half-conversion times longer than a few years under our experimental conditions.

It must be emphasized that the electron transfers in eqs 3–8 only scramble the charges of the species in the diffusion layer; they cannot at all alter the local overall content in *cis* or *trans* species.[22] Therefore, they alone cannot be responsible for the nonmonotonous variations of $\varrho = i_p(trans^{+/0})/i_p(cis^{0/+})$ presented in Figure 2a. This statement is theoretically confirmed by the fact that the working curve shown in Figure 2a, which takes into account all of the above homogeneous electron transfers, gives rise to monotonous variations as a function of the scan rate.

Figure 2b presents a set of working curves predicting the variations of ϱ as a function of the dimensionless parameter $k_1(RT/Fv)$, for several values of the reciprocal equilibrium constant (*viz.* $1/K^{2+} = k_2/k_1$) of the cis^{2+} to $trans^{2+}$ isomerization step considered in Scheme 3:

$$cis^{2+} \underset{k_2}{\overset{k_1}{\rightleftharpoons}} trans^{2+} \quad K^{2+} = k_1/k_2 \quad (9)$$

This set of working curves matches qualitatively the experimental variations observed in Figure 2a. Thus, for the larger scan rates, ϱ decreases as the scan rate is increased in agreement with expected variations since less and less $trans^{2+}$ species is formed during the shorter

(19) On the basis of Marcus (or Hush-Marcus) theory,[18] there is a direct relationship between the activation energies of heterogeneous and homogeneous electron transfer involving the same redox couples. Therefore, fast heterogeneous electron transfers correspond to homogeneous electron transfers that are expected to be under activation control only within a limited energetic window located around $\Delta G° = 0$. Outside of this gap, the electron-transfer rate constants are diffusion-controlled by diffusion of the products ($\Delta G° > 0$) or the reactants ($\Delta G° < 0$). Thus, one has $k_f \approx k_{diff}/[1 + \exp(\Delta G°/RT)]$ and $k_b \approx k_{diff}/[1 + \exp(-\Delta G°/RT)]$, respectively, for the forward and backward rate constants (with obviously $k_f/k_b = \exp(-\Delta G°/RT)$). For a more extended discussion of these points see refs 18 and 20.

(20) Schlesener, C. J.; Amatore, C.; Kochi, J. K. *J. Am. Chem. Soc.* **1984**, *106*, 3567.

(21) The homogeneous electron transfers are necessarily bimolecular. Therefore, a concentration dependence is expected despite the first-order kinetics of the isomerization reactions in Scheme 3. However, due to the fact that they correspond to rates that are much larger than those of the isomerization process, they cannot be rate determining.[22]

(22) These electron transfers are generally unnoticeable when they involve chemically reversible redox couples, although they perturb drastically the concentration profiles of the species in the diffusion layer.[23,24] However, their involvement is revealed when the symmetry of Fick's second law is broken due to the involvement of chemical kinetic terms (as happens here)[23] or other transport terms such as migration.[24]

(23) For experimental evidence of the role of homogeneous electron transfers when chemical kinetics are involved, see *e.g.*: (a) Amatore, C.; Chaussard, J.; Pinson, J.; Savéant, J.-M.; Thiébault, A. *J. Am. Chem. Soc.* **1979**, *101*, 6012. (b) Amatore, C.; Pinson, J.; Savéant, J.-M.; Thiébault, A. *J. Electroanal. Chem. Interfacial Electrochem.* **1980**, *107*, 59. (c) Amatore, C.; Pinson, J.; Savéant, J.-M.; Thiébault, A. *J. Electroanal. Chem. Interfacial Electrochem.* **1980**, *107*, 75. (d) Amatore, C.; Savéant, J.-M. *J. Electroanal. Chem. Interfacial Electrochem.* **1980**, *107*, 353. (e) Zizelman, P. M.; Amatore, C.; Kochi, J. K. *J. Am. Chem. Soc.* **1984**, *106*, 3771.

(24) For experimental evidence of the role of homogeneous electron transfers upon introducing migrational transport terms (*viz.* by decreasing the ionic strength) see: (a) Norton, J. D.; Benson, W. E.; White, H. S.; Pendley, B. D.; Abruña, H. D. *Anal. Chem.* **1991**, *63*, 1909. (b) Norton, J. D.; White, H. S. *J. Electroanal. Chem. Interfacial Electrochem.* **1992**, *325*, 341. (c) Bento, F.; Montenegro, I.; Amatore, C. Unpublished results (1993): manuscript in preparation.

and shorter time durations in which the electrode potential is on the plateau of the $cis^{+/2+}$ wave. Within this zone, the effect of the backward reaction (*viz.* of k_2/k_1) is almost negligible. Conversely, for the smallest scan rates, ϱ increases as the scan rate is increased, and the effect of the backward reaction (*viz.* of k_2/k_1) is determinant. This theoretical behavior is rationalized through the following consideratins. When the potential is lying on the plateau of the $cis^{+/2+}$ wave, the $trans^{2+}$ species is produced, and provided eq 9 is exergonic enough, the backward rate constant plays almost no kinetic role. However, during the backward potential scan, while the potential is scanned over the range lying between the cis^{2+} and the $trans^{2+}$ reduction waves, the equilibrium in eq 9 is continuously displaced toward its left-hand side by the electrode.[25] Indeed, the cis^{2+} isomer then becomes unstable at the electrode surface, being reduced into cis^{+}, while the $trans^{2+}$ isomer remains unaffected. This forces the isomerization to proceed backwards, to an extent that depends mainly on k_2, the backward rate constant value. As soon as the $trans^{2+}$ reduction wave is scanned over, this effect ceases since the equilibrium in eq 9 is then pulled almost equivalently on both directions by the simultaneous reductions of the cis^{2+} and $trans^{2+}$ isomers into their monocationic forms. Furthermore, since the concentrations of both species involved in the equilibrium kinetics are destroyed by their reduction, the *cis/trans* composition of the diffusion layer is electrochemically "quenched". In other words, eq 9 can never recover its equilibrium situation, *viz.*, the equilibrium that was almost achieved when the potential was on the plateau of the $cis^{+/2+}$ wave, and remains in an "out-of-equilibrium" state. This "out of equilibrium" state (except for interference of diffusion as described above and discussed below) is examined later on when the potential is scanned over the reduction waves of the monocations. It is therefore clear that the effect of the backward isomerization in eq 9 can take place only over a limited potential window ΔE, on the order of $E°(cis^{2+/+}) - E°(trans^{2+/+})$, and thus only over a limited time duration $\theta \approx \Delta E/v$. Since $k_2\theta$ must be sufficiently large for any significant kinetic effect to be observed, observation of values of ϱ that deviate significantly from the predictions of the working curve shown in Figure 2a (*viz.* from a situation where $k_2 = 0$) requires the scan rate to be below a threshold value that depends on ΔE, k_1, and k_2.[26] Moreover, beyond this threshold value, the smaller the scan rate and the larger the k_2 value, the larger $k_2\theta$ is, and therefore the larger the deviation is, in agreement with the theoretical predictions in Figure 2b and the experimental observations in Figure 2a.

The fits shown in Figure 2c illustrate the excellent quantitative agreement between the theoretical predictions based on Scheme 3 and on the series of homogeneous electron transfers in eqs 3−8 (Figure 2b) and the experimental data in Figure 2a. The best fits are obtained for $k_1 = 5.6 \pm 0.3$ s^{-1} and $1/K^{2+} = k_2/k_1 = 0.18 \pm 0.01$, *viz.* $k_2 = 1.0 \pm 0.1$ s^{-1}.

On the basis of this set of values, one may consider it rather puzzling that the electrochemistry of the $trans^0$ consists of a set of two reversible waves as described above. Indeed, provided that the scan rate is not too large, the same equilibrium between the $trans^{2+}/cis^{2+}$ species is expected to be achieved when the potential is located on the plateaus of the $trans^{+}$ and cis^{+} oxidation waves, whether one starts from a *cis* or a *trans* solution. Thus, it is deduced that some cis^{2+} (*ca.* 15% at equilibrium) must be formed on the plateau of the second oxidation wave of a pure $trans^0$ solution. Moreover, this equilibrium should also be displaced uphill (*viz.* toward the *cis* isomer) when the reduction wave of cis^{2+} is scanned over as described above. On the basis of such considerations, a cis^{+} reduction wave should also be observed in the voltammetry of a pure $trans^0$ solution as soon as the second oxidation wave is scanned over for the range of scan rates investigated here. However, this simple reasoning does not take into account the alteration by diffusion of the solution content in the electrode vicinity (*vide supra et infra*). We have already explained above and will discuss more thoroughly below how diffusion tends to restore a solution composition close to that prevailing in the bulk while the potential is scanned over the gap separating the 2+/+ and +/0 reduction waves. When one starts from a cis^0 solution, this effect leads to a reduction wave for the cis^{+} cation larger than that expected from the actual extent of backward isomerization. Conversely, when one starts from a $trans^0$ solution, the would-be observable reduction wave of the cis^{+} cation becomes vanishingly small because the bulk solution now contains only the *trans* isomer (*vide infra* and Figure 3a).

Because $\Delta G° = 0$ for each thermochemical cycle represented by the squares in Scheme 2, one has

$$0 = RT \ln (K^{2+}/K^{+}) - F[E°(cis^{2+/+}) - E°(trans^{2+/+})] \quad (10)$$

$$0 = RT \ln (K^{2+}/K^{0}) - F[E°(cis^{+/0}) + E°(cis^{2+/+}) - E°(trans^{2+/+}) - E°(trans^{+/0})] \quad (11)$$

Since the equilibrium constant ($K^{2+} = 5.6$) of the isomerization between the dications in eq 9 is known, this allows us to evaluate the formal equilibrium constants $K^0 = 6.9 \times 10^{-4}$ and $K^{+} = 1.5$ of the corresponding reactions for the neutral or monocationic species, respectively. This will indeed permit us to decide if these reactions do not occur because of thermodynamic or kinetic reasons. The K^0 value establishes that the $trans^0$ isomer is thermodynamically unstable by *ca.* 4 kcal/mol with respect to the cis^0 isomer, showing that formation of the former species can occur only under kinetic control. Conversely, the $trans^{+}$ isomer is slightly more stable than the cis^{+} one (by *ca.* 0.2 kcal/mol). However, no hint of any $cis^{+}/trans^{+}$ interconversion could be obtained in the electrochemical study, either by cyclic voltammetry, since both $cis^{0/+}$ and $trans^{0/+}$ waves are perfectly chemically reversible even at the lowest scan rates (0.05 V s^{-1}) used in this work, or by CPE experiments, since solutions of cis^{+} or $trans^{+}$

(25) This is akin to a CE (*C*hemical + *E*lectrochemical)[14] electrochemical mechanism taking place at the cis^{2+} complex reduction wave. However, the characteristic plateau wave is not apparent due to the partial merging of this wave with that of the $trans^{2+}$ complex. For a similar situation see *e.g.*: (a) Amatore, C.; Jutand, A.; Khalil, F.; M'Barki, M. A.; Mottier, L. *Organometallics* **1993**, *12*, 3168. For the theory of "classical" CE behavior,[14] see *e.g.*: (b) Savéant, J.-M.; Vianello, E. *Electrochim. Acta* **1963**, *8*, 905. (c) Nicholson, R. S.; Shain, I. *Anal. Chem.* **1964**, *36*, 706.

(26) k_1 still plays a major role, since the forward reaction tends to oppose the uphill displacement of the equilibrium in eq 9 by the electrode. In fact, the overall phenomenon depends on the dimensionless parameter $(k_2/k_1)[(k_1 + k_2)\theta]^{1/2}$,[14,25b,c] However, for a given value of $k_1\theta$ (*e.g.*, as in Figure 2b, where $\theta \propto RT/Fv$) it depends only on $k_2\theta$.

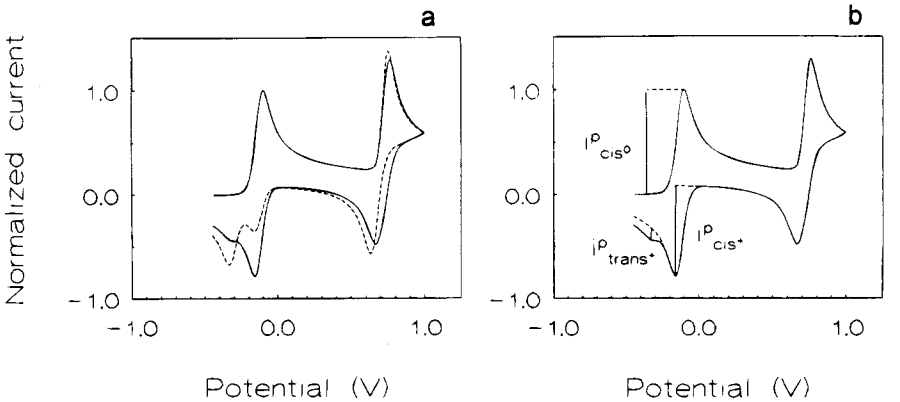

Figure 3. Simulated voltammograms of a cis^0 solution according to the mechanism in Scheme 3 including the homogeneous electron transfer in eqs 3–8 and $k_1RT/Fv = 10$ and $k_2/k_1 = 0.18$ (a, solid line) or 0 (a, dashed line). In (b) the extrapolation curves allowing the measurements of the various currents required for evaluation of $\varrho = i_p(trans^{+/0})/i_p(cis^{0/+}) = i_p(trans^{+/0})/[i_p(trans^{+/0}) + i_p(cis^{+/0})]$ or of the conservation of mass (see text and Experimental Section) are shown in dashed lines. Current scales are normalized relative to the peak current $i_p = 0.446FAC^0(DFv/RT)^{1/2}$ [14] of a Nernstian chemically reversible wave corresponding to identical concentration (C^0), electrode surface area (A), and scan rate (v). Potential scales are expressed in V *vs* SCE for 0 °C.

isomers electrogenerated by oxidation of their neutral precursors remained stable on the time scale of preparative electrolysis, *i.e.* at least 45 min. This indicates that the rate constants relative to the $cis^+/trans^+$ isomerization equilibrium are much below 10^{-4} s^{-1}; *viz.*, they are smaller than those relative to the $cis^{2+}/trans^{2+}$ isomerization (eq 9) by a factor of at least 10 000. Such a figure establishes that the oxidation of the monocations (17-electron species) into the dications (16-electron species) results in a decrease of the isomerization activation barrier by at least 5 kcal/mol. The kinetic gain is then at least 7 times larger than the corresponding thermodynamic gain of only *ca.* 0.7 kcal/mol, since $(\Delta G°)^+ \approx -0.2$ kcal/mol for the cis^+ to $trans^+$ equilibrium as compared to $(\Delta G°)^{2+} \approx -0.9$ kcal/mol for the cis^{2+} to $trans^{2+}$ equilibrium. These figures stress the dramatic increase of structural lability that is brought into the *cis* and *trans* complexes by promotion to their 16-electron configurations upon oxidation.

Quantitative Comparison between the Effects of Diffusion and Backward Isomerization. To conclude this discussion, we wish to illustrate and discuss on more quantitative grounds the effect of diffusion. The simulated voltammogram drawn with a dashed line in Figure 3a corresponds to $k_1RT/Fv = 10$ and $k_2 = 0$. This set of values was chosen to ensure that the cis^{2+} to $trans^{2+}$ conversion is nearly quantitative during the time in which the potential is scanned over the range corresponding to the plateau of the $cis^{+/2+}$ wave and that no backward isomerization may occur. Proof of this statement is given by the sharp reduction wave observed around 0.65 V that features the exclusive reduction of the $trans^{2+}$ species without any significant interference from the reduction of traces of the residual cis^{2+} isomer. Despite such evidence for complete conversion, it is seen that a rather large reduction wave is observed for reduction of the cis^+ species, whereas that observed for reduction of the $trans^+$ species is smaller than that observed for reduction of its $trans^{2+}$ parent. Thus, on the basis of the examination of the set of $cis^{2+}/trans^{2+}$ reduction waves the conversion is found to be nearly 100%, whereas it appears to be in the range of only 50% on the basis of the examination of the set of $cis^+/trans^+$ reduction waves. This apparent contradiction allows us to quantify the effect of diffusion removal/replenishment of the diffusion layer that occurs while the potential is scanned between the two sets of waves.[16] Thus, during the time delay between the two "measurements" (*viz.* that at the level of the dications and that at the level of the monocations) *ca.* 50% of the *trans* species formed has been removed from the vicinity of the electrode by diffusion toward the bulk of solution; simultaneously, this process was compensated by diffusion of an equivalent amount of cis^0 species from the solution bulk toward the electrode. Since the cis^0 species is electrochemically unstable in this range of potential, it is converted to its cis^+ product as soon as it reaches the electrode surface.

This alteration of the diffusion layer content can only result from diffusion, since the dashed voltammogram in Figure 3a was simulated with $k_2 = 0$, thus preventing any backward isomerization from taking place. Conversely, the voltammogram represented by the solid line in Figure 3a corresponds to the same value of $k_1RT/Fv = 10$ as the dashed one but incorporates a backward isomerization step such as $k_2/k_1 = 0.18$, *viz.* using the same value as determined above for the experimental system investigated here. Therefore, comparison of the two voltammograms in Figure 3a illustrates quantitatively the effects of the backward isomerization. Thus, the fact that the backward isomerization does not play any important role when both cis^{2+} and $trans^{2+}$ species are stable at the electrode is demonstrated by the near-identity of the simulated waves (*viz.* dashed and solid ones) featuring the oxidation of the cis^+ species. Conversely, the corresponding reduction waves are significantly different due to the backward isomerization, since when $k_2 \neq 0$ (solid voltammogram) reduction of the cis^{2+} species at the electrode surface results in an uphill but continuous displacement of the equilibrium in eq 9 toward its left-hand side. Although the resulting effect is difficult to quantify at the level of the cis^{2+} and $trans^{2+}$ overlapping reduction waves, it is easily apparent at the level of the cis^+ and $trans^+$ reduction waves. Indeed, the difference between the dashed voltammogram (effect of diffusion alone) and the solid one (effect of backward isomerization and diffusion) gives a measure of the extent to which the isomerization equilibrium in eq 9 has been pulled uphill toward its left-hand side during the period in which the cis^{2+} and $trans^{2+}$ waves have been scanned over.

Final Comments. The dependence of the relative stability of geometrical isomers of octahedral-type complexes on the electronic configuration has been a matter of recognized interest[1-9] but is not yet clearly understood, in particular for closed-shell phosphine complexes with two π-acceptor or two π-donor ligands and their derived 17- or 19-electron species.

This work extends the investigation to complexes with one π-acceptor (nitrile) and one π-donor (chloride) ligand, from the 18-electron down to the 16-electron configuration, situations which do not appear to have been previously considered; moreover, it provides the first detailed kinetic and mechanistic study of the involved isomerization reactions induced by electron transfer. It establishes that (i) for the closed-shell complexes the *cis* isomer is substantially more stable than the *trans* isomer and that (ii) although a single-electron oxidation of such species can lead to a high increase of the relative thermodynamic stability of the *trans vs* the *cis* isomer, kinetic effects may require a second oxidation step (with a concomitant dramatic kinetic gain but a rather modest thermodynamic one) to allow a significant *cis* to *trans* isomerization to occur within the usual electrochemical time scale.

Moreover, the possibility of further occurrence, in the electrochemical process, of the reverse isomerization has also been demonstrated. Indeed, although the backward isomerization (*trans*$^{2+}$ to *cis*$^{2+}$) is endergonic, it occurs under electrochemical conditions because it is driven by reduction of the *cis*$^{2+}$ isomer at the electrode surface that continuously shifts the isomerization equilibrium uphill.

Experimental Section

Chemicals and Instrumentation. All the reactions were carried out in the absence of air using standard inert-gas flow and vacuum techniques. IR spectra were recorded on a Perkin-Elmer 683 spectrophotometer and ^{1}H and ^{31}P{^{1}H} NMR spectra on a Varian Unity 300 spectrometer; proton chemical shifts are reported from Me_4Si, and phosphorus chemical shifts are relative to $P(OMe)_3$.

Solvents were purified by standard procedures, and NCC_6H_4-Me-4 was used as purchased from Fluka. *trans*-[ReCl(N_2)-(dppe)$_2$][27] and *trans*-[ReCl(NCC_6H_4Me-4)(dppe)$_2$][28] (IR (KBr pellet; cm^{-1}) ν(NC) 2050 (m); ^{1}H NMR (CD_2Cl_2) δ 2.30 (s) (CH_3); ^{31}P{^{1}H} NMR (CD_2Cl_2) δ −115.9, relative to $P(OMe)_3$) were prepared as previously described. Other complexes were obtianed as follows.

***cis*-[ReCl(NCC_6H_4Me-4)(dppe)$_2$].** NCC_6H_4Me-4 (0.270 g, 2.30 mmol) was added to a stirred solution of *trans*-[ReCl(N_2)-(dppe)$_2$] (1.14 g, 1.09 mmol) in toluene (900 cm^3) under argon; the system was irradiated by a tungsten-filament light (100 W bulb at *ca.* 15 cm distance) for *ca.* 0.5 h, and then the mixture was stirred under ambient light conditions for 4 days. Concentration *in vacuo* with slight heating (*ca.* 50 °C) led to the precipitation of *cis*-[ReCl(NCC_6H_4Me-4)(dppe)$_2$] as an orange solid, which was filtered off, washed with a 1:2 mixture of toluene/hexane, and dried *in vacuo*. Further crops could be obtained from the mother liquor by following similar concentration procedures; total yield *ca.* 0.85 g (75%). IR (KBr pellet; cm^{-1}): ν(NC) 2175 (m). ^{1}H NMR (C_6D_6): δ 2.34 (s) (CH_3). ^{31}P{^{1}H} NMR (C_6D_6; ABCD-type spin system; δ relative to $P(OMe)_3$): δ_A −114.80, δ_B −112.53, δ_C −107.16, δ_D −105.40; J(AB) = 13.8, J(AC) = 6.5, J(AD) = 0.5, J(BC) = 215.3, J(BD) = 13.9, J(CD) = 6.2 Hz. Anal. Calcd (found) for $C_{60}H_{55}NP_4ClRe \cdot {}^1/_2C_7H_8$: C, 64.5 (64.5); H, 5.3 (5.0); N, 1.2 (1.2).

***trans*-[ReCl(NCC_6H_4Me-4)(dppe)$_2$][PF_6].** [Et_3O][PF_6] (0.21 g, 0.83 mmol) was added to a stirred and cooled (*ca.* −63.5 °C) solution of *cis*-[ReCl(NCC_6H_4Me-4)(dppe)$_2$] (0.40 g, 0.35 mmol) in CH_2Cl_2 (30 cm^3). The solution was slowly warmed to room temperature and, after *ca.* 12 h, concentrated *in vacuo*, and upon addition of Et_2O, the oxidized product *trans*-[ReCl(NCC_6H_4-Me-4)(dppe)$_2$][PF_6] precipitated as an orange solid which was filtered off and washed with CH_2Cl_2/Et_2O. Further crops were obtained from the mother liquor, by concentration and addition of Et_2O; they were recrystallized from CH_2Cl_2/Et_2O. Total yield: 0.34 g (75%). IR (KBr pellet; cm^{-1}): ν(NC) 2130(m). The compound is paramagnetic. Anal. Calcd (found) for $C_{60}H_{55}NP_5F_6ClRe$: C, 57.5 (58.0); H, 4.7 (4.5); N, 1.3 (1.1).

Cyclic voltammograms were obtained at 0 °C, in 0.2 mol dm^{-3} solutions of [Bu_4N][BF_4] in THF, at a platinum-disk working electrode (0.5 mm diameter) whose potential was controlled *vs* a Luggin capillary connected to a silver wire pseudo reference electrode; a Pt auxiliary electrode was employed. An EG&G PARC 175 universal programmer and an EG&G PARC 173 potentiostat/galvanostat or a HI-TEK PP RI wave form generator and a HI-TEK DT 2101 potentiostat/galvanostat were used. The voltammograms were recorded on a Linseis LY 1600 or Philips PM 8043 X-Y recorder.

Controlled-potential electrolyses (CPE) were carried out in electrolyte solutions with the above-mentioned composition, in a three-electrode H-type cell. The two compartments were separated by a glass frit and equipped with platinum gauze working and counter electrodes. A Luggin capillary connected to a silver wire pseudo reference electrode was used to control the working electrode potential. All manipulations were carried out under dinitrogen. The redox potentials of the complexes are given in volts *vs* SCE and determined by using as a postcalibration internal reference the *trans*-[ReCl(N_2)-(dppe)$_2$]$^{0/+}$ couple (E° = 0.280 V *vs* SCE).

Measurement of ϱ Values in Figure 2. The determination of ϱ values reported in Figure 2 was rather delicate in both experimental and theoretical voltammograms. The principle of the measurement of the various currents that are required for the determination of ϱ values and check of the mass conservation (see text) is shown by the simulated voltammogram in Figure 3b. It is seen that the most difficult measurement is that of i_p(*trans*$^{+/0}$), since it corresponds to the maximum value of the difference between the true current (solid line) and the extrapolation of the diffusion current (dashed line) corresponding to the plateau of the *cis*$^+$ reduction wave. Due to the small experimental values of i_p(*trans*$^{+/0}$)/i_p-(*cis*$^{+/0}$) this procedure required a precise extrapolation of the diffusional current of the *cis*$^+$ reduction wave. This was performed by simulating an extended set of voltammograms corresponding to the two *cis* redox couples alone (*viz.* using the program described in the following with $k_1 = k_2 = 0$ and neglecting the homogeneous electron transfers in eqs 3−8), for various concentrations of the *cis*^{0} reactant. Thus, for any experimental voltammogram, a simulated voltammogram with a *cis*$^+$ reduction wave exactly superimposable on the rising portion and peak range of the experimental one was available. The diffusion current of the experimental *cis*$^+$ reduction wave could then be extrapolated with good precision by reporting that of the matching simulated voltammogram. To check any systematic error, the same procedure was used to determine the theoretical r values (used in Figure 2b) by using simulated voltammograms (*i.e.*, those obtained for any k_1 and k_2 values, considering the homogeneous electron transfers in eqs 3−8) instead of experimental ones. These values compared satisfactorily (within 2% relative error) with the true theoretical values of i_p(*trans*$^{+/0}$) that were directly available from the simulation program. Thus, this procedure introduced much lower errors than other experimental factors (mainly due to

(27) Chatt, J.; Kan, C. T.; Leigh, G. J.; Pickett, C. J.; Stanley, D. R. *J. Chem. Soc., Dalton Trans.* **1980**, 2032.
(28) Pombeiro, A. J. L.; Silva, M. F. C. G.; Hughes, D.; Richards, R. L. *Polyhedron* **1989**, *8*, 1872.

reproducibility and estimation of background currents), as shown by the error bars given in the top right-hand side of Figure 2a,c.

Derivation of the Working Curves in Figure 2b. The working curves in Figure 2b were determined along classical explicit finite difference procedures,[14] using Turbo-Pascal 5.0 programming. The chemical isomerization steps having relatively small rate constants could be taken into account by classical procedures (*i.e.*, *via* approximation of the chemical terms through Taylor–Young first-order developments).[14] However, the rate constants of the extremely rapid electron-transfer steps in eqs 3–8, being close to the diffusion limit, were too large to be treated along such procedures without requiring infinite computational times and memory occupations. Two different procedures were used according to the reversible or irreversible nature of these steps. At any point of the solution and any time, the kinetic effect of the irreversible reactions (5–8) is to annihilate the species considered in their left-hand side that has the smallest local concentration. This results in a segregation of the species in different zones of the diffusion layer.[24] Therefore, each of these reactions was replaced by a comparator algorithm that (i) evaluated at each node of the space–time grid the reactant with the smallest concentration value, (ii) subtracted this value from the concentration of the other reactant, and (iii) added this value to the concentration of each species in the right-hand side of the corresponding reaction (step i accounts for the annihilation, while steps ii and iii account for the mass conservation). After these comparator algorithms had been performed, the fast reversible electron transfers (eqs 3 and 4) were accounted for. This was done by forcing simultaneously (at each node of the space–time grid) the two mass action laws of reactions 3 and 4 at their equilibrium values; evaluation of the corresponding concentration changes for each species allowed us to modify their concentrations accordingly. After the two series of electron transfers were taken into account by the two different procedures above, the effects of the relatively slow chemical isomerizations were taken into account classically as described above. Nernstian electrode boundary conditions were used and programmed classically; individual currents and fluxes were evaluated using parabolic expansions. All of the programming was performed using dimensionless parameters. Source files for Turbo-Pascal 5.0 or executable files are available upon request to one of the authors (C.A.).

Acknowledgment. This work was partially supported by the JNICT (The National Board for Scientific and Technological Research) and the INIC (The National Institute for Scientific Research) of Portugal, as well as by the CNRS (Centre National de la Recherche Scientifique) and the ENS (Ecole Normale Supérieure) of France. A joint CNRS–JNICT international grant is also acknowledged.

OM940160H